ELSEVIER

Journal of Molecular Catalysis A: Chemical 168 (2001) 279–287

JOURNAL OF MOLECULAR CATALYSIS A: CHEMICAL

www.elsevier.com/locate/molcata

Gas-phase hydrogenation of acetonitrile over nickel supported on alumina- and mixed alumina/gallium oxide-pillared tin phosphate catalysts

P. Braos-García, P. Maireles-Torres, E. Rodríguez-Castellón, A. Jiménez-López*

Departamento de Química Inorgánica, Cristalografía y Mineralogía, Facultad de Ciencias, Universidad de Málaga, Campus de Teatinos, 29071 Málaga, Spain

Received 4 August 2000; accepted 8 November 2000

Abstract

Gas-phase hydrogenation of acetonitrile has been studied by using catalysts based on nickel supported on alumina- and mixed alumina/gallium oxide-pillared tin phosphate materials. The in situ thermal decomposition of nickel formate has demonstrated to be an interesting method to obtain dispersed nickel particles on pillared tin phosphate supports. These catalysts are active in this catalytic reaction, but all the catalysts exhibit important deactivation. The study of the influence of the structural and acid properties of the catalysts on their catalytic performance allows us to establish that both hydrogenation and condensation reaction leading to higher amines take place on the metal particles.

Keywords: Hydrogenation of acetonitrile; Supported nickel catalysts; Pillared solids; Layered metal phosphate; Tin hydrogenphosphate

1. Introduction

Hydrogenation of nitriles is an alternative method to produce amines instead of the classical reactions between ammonia and an alcohol or an aldehyde or ketone in the presence of hydrogen over hydrogenation catalysts, but which need high temperatures and pressures [1,2]. The lower aliphatic amines are valuable products widely used in the manufacture of medicinal, agricultural, textile, rubber and plastic chemicals.

Different catalytic systems have been tested for the gas-phase hydrogenation of nitriles [3–7]. Thus, Verhaak et al. [5] have reported the influence of the support acidity of nickel based catalysts on the selectivity in the hydrogenation of acetonitrile. These authors found that nickel supported on basic supports were highly selective towards the formation of the primary amine. However, an influence of the support on the degree of nickel dispersion has been also claimed to be important in the catalytic performance for this reaction [4]. These researchers also found that the substitution of nickel by platinum shifted the selectivity, giving rise to the secondary amine as the main reaction product [8].

Regarding the mechanism implied in the gas-phase hydrogenation of acetonitrile, Verhaak et al. [5] proposed a bifunctional mechanism where the active sites for the hydrogenation are located on the metal, and the acid function which catalyzes the transamination reaction leading to secondary and tertiary amines are situated on the support. However, other authors [3,9]

* Corresponding author. Tel.: +34-952-131876; fax: +34-952-132000.
E-mail address: ajimenezl@uma.es (A. Jiménez-López).

1381-1169/01/$ – see front matter
PII: S1381-1169(00)00544-6

point to that all reaction steps converting nitriles to the different amines take place on the catalyst surface.

On the other hand, the family of pillared layered solids (PLS) has been extensively studied due to the need of porous solids with larger pore sizes than those of microporous zeolites, which could be able to catalyze voluminous species such as those present in the heavy fraction of petroleum [10]. In the case of pillared layered phosphates, they are obtained by the insertion of inorganic oligomeric species in the interlayer region of metal(IV) phosphates and subsequent thermal treatment, a process which leads to nanostructured materials, where the presence of the corresponding metal oxide nanoparticles, acting as pillars, facilitates the access to the interlayer region of different reactants [11]. This pillaring process gives rise to porous solids which structural and chemical features can be tailored by suitable choosing of the layered inorganic material, the metal oxide precursor and the pillaring conditions. These solids have demonstrated to be active, for instance, in the dehydrogenation of light alkanes [12], as support for the hydrodesulfuration of thiophene [13].

Therefore, it is clear that catalysts based on pillared layered metal phosphates could be potential candidates for the catalytic hydrogenation of nitriles. In the present paper, we have used the hydrogenation of acetonitrile as a model reaction to study the catalytic properties of nickel supported on alumina- and mixed alumina-gallium oxide pillared tin phosphate with different Ni percentages. In order to obtain metallic nickel particles of reduced size, the thermal decomposition of samples impregnated with nickel formate aqueous solution has been used.

2. Experimental

Two different supports, alumina and mixed gallium/alumina oxide pillared tin phosphates (AlSnP and GaAlSnP, respectively), have been impregnated with nickel species. These supports were synthesized as described elsewhere [14], but they were calcined in air at 773 K for 8 h. The catalyst precursors containing different wt.% Ni loadings (10, 15 and 20) were prepared by using the incipient wetness impregnation with a nickel formate ammonia solution. Then, the Ni^0 supported catalysts were obtained by the in situ thermal decomposition of the precursors at 598 K. This process leads to the decomposition of the nickel formate with the subsequent reduction of nickel(II) to Ni^0. The catalysts will be, hereafter, designated as Al-Ni*x* and GaAl-Ni*x*, where *x* is the wt.% of Ni.

In order to study the influence of the intrinsic acid properties of the support on the catalytic performance, potassium exchanged supports have been also prepared by treating the ammonium form with an aqueous solution of potassium acetate. In this way, potassium contents of 0.98 and 1.05 wt.% were attained with the Al-SnP and GaAl-SnP supports, respectively. After incorporating the nickel species, the catalysts labeled as AlK-Ni20 and GaAlK-Ni20 were obtained.

Chemical analysis of catalysts were carried out after treatment with concentrated HNO_3 aqueous solution. After filtration, Ni and K were determined by atomic absorption using a Perkin-Elmer 400 spectrometer.

The X-ray photoelectron spectra (XPS) were recorded with a Physical Electronics 5700 instrument provided with a multichannel hemispherical electron analyzer, the band-pass energy being 29.35 eV. The Mg Kα X-ray excitation source ($h\nu = 1253.6$ eV) was at a power of 300 W and the pressure in the analysis chamber was maintained below 1.3×10^{-7} Pa during data acquisition. The binding energies (BE) were obtained with ±0.2 eV accuracy and charge compensation was done with the adventitious C 1s peak at 284.8 eV. Before the XPS study, the precursor were heated at 598 K under a helium flow in a pretreatment chamber, and then displaced into the analysis chamber.

Textural parameters have been extracted from the N_2 adsorption–desorption isotherms at 77 K obtained using a glass conventional volumetric apparatus (catalysts outgassed at 573 K and 10^{-2} Pa overnight).

Temperature-programmed desorption of ammonia (NH_3-TPD) was used to determine the total acidity of the catalysts. Before the adsorption of ammonia at 373 K, the samples were heated at 598 K in a He flow for 90 min. The NH_3-TPD was performed between 373 and 598 K, with a heating rate of 10 K min^{-1}. The evolved ammonia was analyzed by on-line gas chromatograph (Shimadzu GC-14A) provided with a thermal conductivity detector.

The amount of surface nickel atoms on the catalysts was known from hydrogen chemisorption at 298 K and using a conventional volumetric apparatus. About 450 mg of each precursor were decomposed in

situ at 398 K under a flow of helium (heating rate of 10 K min^{-1}). Similarly, the amount of reduced nickel was evaluated by oxygen chemisorption at 673 K.

Before the catalytic studies, all precursors were pressed at 5000 Kg cm^{-2}, crushed and sieved. A sieve fraction of 0.2–0.3 mm was used in all catalytic studies.

The gas-phase hydrogenation of acetonitrile was performed in a flow system operating at atmospheric pressure. A tubular Pyrex reactor (27 cm length, 7 mm O.D. and 3.6 mm I.D.) and 55 mg of precursor were used. Prior to any measurement, the precursors were decomposed in situ, by heating at 598 K under a helium flow for 90 min. The catalysts were then cooled to room temperature under the same helium flow. A hydrogen flow was bubbled through a saturator containing acetonitrile at 273 K, thus, resulting a feed with 4.7 vol.% of acetonitrile, which was introduced into the reactor. The reactants and products were analyzed by an on-line gas chromatograph equipped with a flame ionization detector and a TRB-14 column. Tests were performed between 378 and 418 K, and a total flow rate of 43.6 ml min^{-1}. A series of preliminary experiments consisting in varying the size of the sieve fractions, catalyst mass and gas flow rate at constant space velocity were also carried out in order to discard the existence of diffusional limitations under the used experimental conditions.

3. Results and discussion

3.1. Characterization of catalysts

The textural and acid characteristics of the two porous pillared tin phosphates, used as support for metal nickel particles are summarized in Table 1. In spite of the different chemical nature of the pillaring species, both supports possess similar textural and acidic properties. Thus, for instance, the S_{BET} values are 200 and 191 $m^2 g^{-1}$, respectively.

On the other hand, these solids have been treated with potassium solution in order to decrease their acidity by incorporating potassium species. It has previously been reported that the selectivity in the acetonitrile hydrogenation in gas-phase seems to depend on the acid nature of the support [5]. From values presented in Table 1, it can be inferred that the exchange process strongly affects the textural and acidic properties of both supports, being the BET surface area, the total and the effective acidities drastically reduced. These changes suggest that K^+ species, in addition to neutralize acid sites, could hinder the access of the nitrogen molecules into the smaller pores, hence, reducing both the specific surface area and the microporous volume. Moreover, it can not be discarded that, during the exchange process, potassium cations occupy positions on cut layers, thus, favoring an heterogeneous reordering of the layer packets. As expected, both the total and the effective acidity, measured as the catalytic activity against the conversion of 2-propanol at 493 K are also reduced after K incorporation.

In order to obtain the nickel supported catalysts, the use of typical nickel salts as precursors must be ruled out due to the concomitant reduction of the tin(IV) species present in the support at temperatures as low as 573 K. Thus, the in situ thermal decomposition of nickel formate becomes an alternative to avoid this problem. This method has previously shown to originate well-dispersed nickel particles [15]. The ease of reduction and the nature of the volatile subproducts involved (CO, CO_2, H_2, H_2O and CH_4) theoretically make formate salts excellent metal precursors far better than the metal nitrate or chloride salts typically used. In the case of nickel formate, the decomposition

Table 1
Structural, textural and acidic characteristics of supports

Support	Al_2O_3 (wt.%)	Ga_2O_3 (wt.%)	S_{BET} ($m^2 g^{-1}$)	V_μ ($cm^3 g^{-1}$)	NH_3-TPD (μmol NH_3 m^{-2})	Conversion of 2-propanol (μmol C_3H_6 $g^{-1} s^{-1}$)
AlSnP	35.7	–	191	0.087	8.9	11.2
AlSnP-K	–	–	81	0.030	7.7	3.3
GaAlSnP	25.9	16.0	200	0.086	9.0	10.9
GaAlSnP-K	–	–	127	0.034	10.0	4.9

Table 2
Binding energies (BE), surface atomic ratio and percentage of Ni^0 as determined by XPS

Catalyst	Binding energy (eV)				Ni/(Al + Ga) atomic ratio	Ni^0 (%)
	Sn	Ni^{2+}	Ni^{2+} (sat)	Ni^0		
Al-Ni10	486.9	855.8	861.8	853.1	0.44	12.4
Al-Ni15	486.6	855.8	861.8	853.0	0.93	14.2
Al-Ni20	486.8	855.9	861.8	853.2	1.28	22.2
AlK-Ni20	487.0	856.6	861.5	853.2	1.00	17.6
GaAl-Ni10	487.1	855.9	861.5	852.3	0.54	22.6
GaAl-Ni15	487.1	855.8	861.5	852.4	0.97	22.7
GaAl-Ni20	487.3	855.4	861.3	852.9	2.13	26.7
GaAlK-Ni20	487.1	856.3	861.1	852.7	1.43	17.5

seems to go through the intermediate of a nickel oxide phase.

The X-ray photoelectron spectroscopy has been used to determine the nature of the nickel species present in the catalysts. Table 2 shows the binding energies of the different elements present in the catalysts and the Ni/(Al + Ga) atomic ratio obtained from the XPS analysis. The Sn $3d_{5/2}$ binding energies (486.6–487.3 eV) of the catalysts are similar to those corresponding to the supports (486.5–486.8 eV). According to these results, we can affirm that Sn(IV) is not reduced during the thermal decomposition of the nickel formate. Regarding the Ni 2p XPS spectra (Fig. 1), they exhibit a rather high complexity due to the presence of various satellite structures that are characteristic of defined Ni states and classically assigned to shake-up processes. The XPS spectra show a peak at low binding energy (852.3–853.2 eV) that can be assigned to Ni^0. The signals at higher binding energies (854.5–855.9 and 857.9–858.7 eV) are due to the coexistence of different species of Ni(II) which are not reduced. The percentage of nickel reduced, determined by XPS, range between 12.4 and 26.7%, increasing with the nickel loading. The Ni/(Al + Ga) atomic ratios increased in each series of catalysts with increasing nickel content, but the potassium

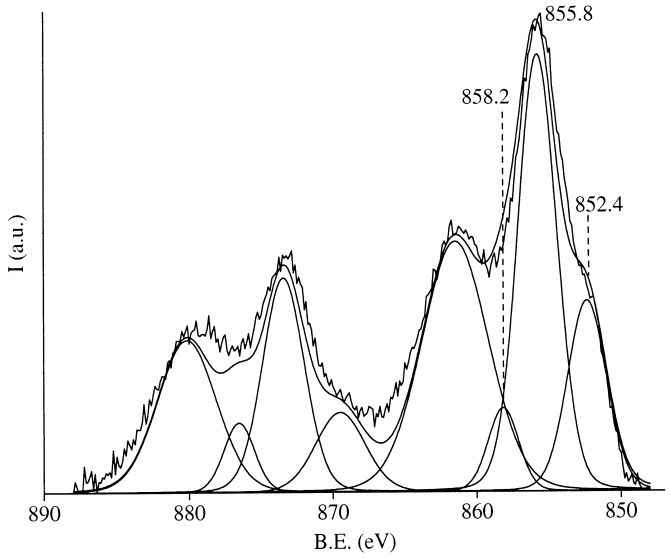

Fig. 1. Cu 2p XPS spectrum of GaAl-Ni15 catalyst.

Table 3
Structural, textural and acidic characteristics of nickel catalysts

Catalyst	Ni (wt.%)	S_{BET} ($m^2\,g^{-1}$)	V_μ ($cm^3\,g^{-1}$)	V_p ($cm^3\,g^{-1}$)	NH_3-TPD (μmol NH_3 m^{-2})
Al-Ni10	10.0	185	0.066	0.154	10.5
Al-Ni15	14.0	188	0.092	0.187	11.1
Al-Ni20	18.4	187	0.086	0.187	12.1
AlK-Ni20	19.2	104	0.047	0.098	9.0
GaAl-Ni10	9.8	188	0.089	0.209	11.9
GaAl-Ni15	14.6	198	0.085	0.206	12.1
GaAl-Ni20	18.4	206	0.090	0.176	10.4
GaAlK-Ni20	18.1	109	0.049	0.117	9.7

exchanged supports lead to both a lower atomic ratio and a lower degree of nickel reduction, as compared with the nickel catalysts prepared with a similar nickel addition (20 wt.%), revealing a better dispersion.

Therefore, under our experimental conditions, an incomplete decomposition of the nickel formate took place. This behavior might be attributed to the strong interaction between the nickel oxide particles and the oxygen rich surface of the support.

Furthermore, the possible formation of nickel aluminate (BE of nickel at 858 eV [16]), after diffusion of nickel into the alumina pillars, would certainly make its reduction more difficult.

The textural characteristics of the nickel containing catalysts (Table 3), compared with those of the corresponding supports, reveal that the incorporation of nickel species barely modifies the S_{BET}, whereas the pore volume is greatly reduced. This fact could be explained by a preferential location of nickel species into the mesopores, because the microporous volume is not very much affected. On the other hand, the total acidity, expressed per surface unit, increases after the nickel incorporation, which seems to indicate that the nickel species can interact with basic ammonia molecules.

Table 4 summarizes the results obtained from hydrogen and oxygen chemisorption. As expected from the XPS results, the reduction degrees obtained from the oxygen chemisorption isotherms indicates that not all the nickel present in the precursors is reduced after the thermal treatment at 598 K. However, these values are higher than those obtained from XPS. The low degrees of nickel reduction lead to an amount of hydrogen chemisorbed very low in all cases. Dispersion data have been calculated assuming a H/Ni stoichiometry of 1, and the amount of hydrogen chemisorbed was deduced from the extrapolation of the isotherm at zero pressure. The dispersion degree varies between 0.7 and 5.6% and, in general, tends to decrease with the nickel content.

Average nickel particle sizes for these catalysts generally range between 3.4 and 42.4 nm, which lead to

Table 4
Properties of the supported nickel catalysts

Catalyst	Ni^0/Ni total (%)	H_2 chemisorbed (μmol H_2 g^{-1})	D (%)	Metal area ($m^2\,g_{Ni}{}^{-1}$)	d (nm)	
					H_2	TEM
Al-Ni10	28.7	13.5	5.6	36.2	3.4	4–6
Al-Ni15	37.4	5.7	1.3	8.3	19.5	20–30
Al-Ni20	47.4	5.5	0.7	4.8	42.4	30–47
AlK-Ni20	43.8	12.5	1.7	11.3	16.7	12–24
GaAl-Ni10	24.9	10.2	4.9	31.7	3.4	4–10
GaAl-Ni15	34.1	8.6	2.0	13.2	11.2	10–30
GaAl-Ni20	43.5	5.2	0.8	5.0	37.8	35–55
GaAlK-Ni20	49.1	12.1	1.6	10.3	20.5	8–35

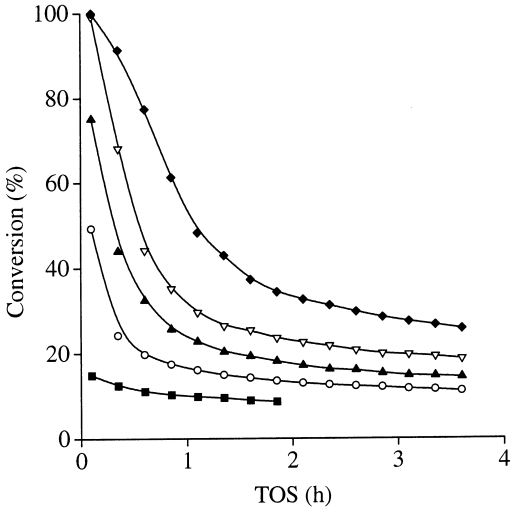

Fig. 2. Variation of conversion in the gas-phase hydrogenation of acetonitrile as a function of time on stream (TOS) on catalyst Al-Ni20 at different reaction temperatures: 378 K (■), 388 K (○), 398 K (▲), 408 K (▽), and 418 K (◆).

metal surface varying between 4.8 and 36.2 $m^2\ g_{Ni}{}^{-1}$. Both series of catalyst follow the same trend as a function of the nickel content. In general, the GaAl-SnP support exhibits a higher capacity to disperse the nickel species, thus, generating smaller metal particles, which can be due to a stronger interaction with this support.

3.2. Catalytic results

Concerning the catalytic performance of the nickel containing alumina and mixed alumina/gallium oxide pillared tin phosphates in the gas-phase hydrogenation of acetonitrile, the main reaction products were, in all cases, ethylamine (EA), diethylamine (DEA) and triethylamine (TEA). In Fig. 2, the acetonitrile conversion on the Al-Ni20 catalyst as a function of time-on-stream (TOS) at different reaction temperatures is presented. The initial acetonitrile conversion increases with the temperature, and a value of 100% is already reached at 408 K. A similar behavior has been reported by Medina-Cabello et al. [17] by using nickel-based catalysts prepared from hydrotalcite-like precursors. However, all catalysts suffer from a severe deactivation, which is more pronounced for higher initial conversion levels (Table 5). A high temperature also favors the desorption of EA and DEA from the active sites, so increasing the selectivity to both amines, and impeding the condensation reactions leading to TEA (Fig. 3). However, if we consider the acid–base interactions between the support and the different molecules present in the reaction media, as well as the basic character of the different amines (EA < TEA < DEA, [18]), it would be expected that EA would be firstly desorbed, thus, decreasing the selectivity toward the higher amines. Nevertheless, the data obtained in this work point to an initial desorption of the DEA as the temperature increases from the active sites, precluding the acid centers located on the support to be the active sites.

The study of the catalytic performance as a function of the nickel content, at a reaction temperature of 398 K, reflects that after few minutes of TOS, the higher is the Ni content, more active is the catalyst (Fig. 4). This evolution agrees with the results reported by Rode et al. [4], which found a lower catalytic

Table 5
Catalytic properties of the supported nickel catalysts in the hydrogenation of acetonitrile at 398 K

Catalyst	Rate (μmol $g^{-1}\ s^{-1}$)		Conversion after 5 min TOS (mol%)	Product selectivity (mol%)[a]		
	5 min TOS	36 min TOS		EA	DEA	TEA
Al-Ni10	13.3	6.3	53.9	54.2	44.0	1.8
Al-Ni15	19.3	7.5	75.9	59.9	39.6	0.5
Al-Ni20	18.9	8.2	75.1	63.2	36.0	0.8
AlK-Ni20	25.5	15.9	100	66.9	33.1	0.0
GaAl-Ni10	2.5	2.3	9.8	55.6	41.6	2.8
GaAl-Ni15	4.4	3.4	17.5	58.0	40.3	1.7
GaAl-Ni20	7.8	4.0	31.7	65.0	34.4	0.6
GaAlK-Ni20	22.0	7.9	89.3	65.2	34.4	0.4

[a] At a conversion level of 13.5%, except for sample GaAl-Ni10 which is 9.8%.

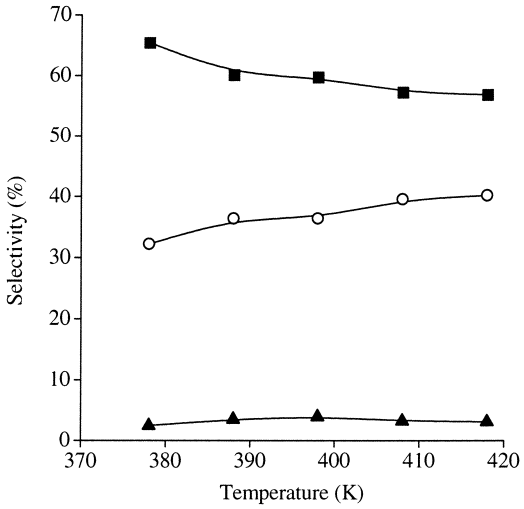

Fig. 3. Influence of reaction temperature on the selectivity of hydrogenation of acetonitrile over catalyst Al-Ni20: EA (■), DEA (○), and TEA (▲).

activity for high dispersion degree, suggesting that this catalytic reaction is structure sensitive. In both series of catalysts, initial conversions superior to 80% are only reached on the potassium containing catalysts. After 3 h of TOS, the conversion values of the different catalysts are, in all cases, comprised between 10 and 20%. However, more important differences are found regarding the selectivity values. It is observed in Table 5, that at 13.5% of conversion, the main reaction product is the EA with a selectivity >54%, whereas the formation of TEA is limited to values <3%.

Several attempts have been carried out in order to regenerate the initial catalytic activity of the Al-Ni20. However, the treatment under a flow of hydrogen at 598 K completely deactivated the catalyst, whereas helium flowing barely affects its catalytic performance. This finding is the opposite of what it has been observed with nickel-on-silica catalysts [19] where the catalytic activity is fully restored after hydrogen treatment at 523 K. In order to get insight into the deactivation process, a spent catalyst has been characterized. Chemical analysis indicate the presence after catalysis of 1.1% C, and a BET surface area of 130 $m^2\,g^{-1}$. From the characterization results (chemical analysis and textural properties), it may be inferred that during catalysis some carbonaceous species are deposited on the surface of the catalysts and blocks

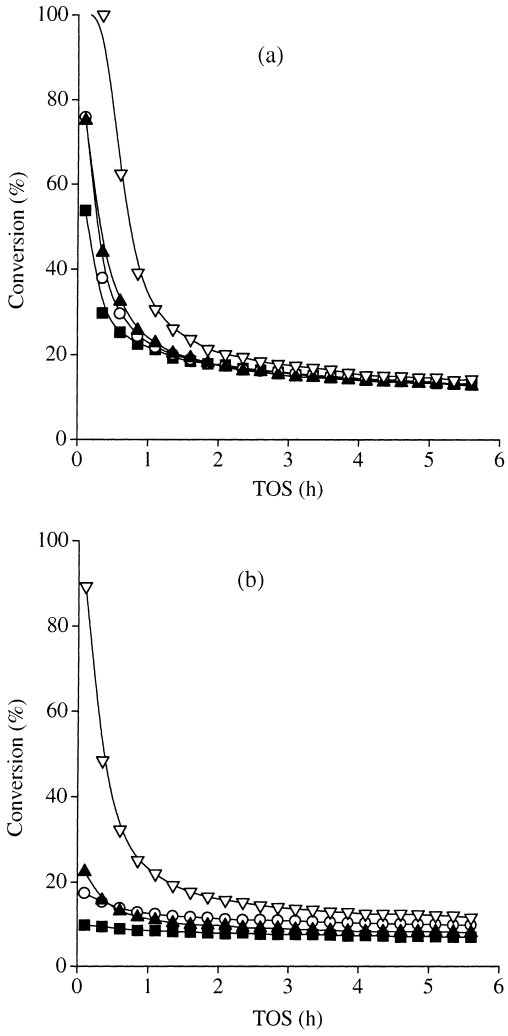

Fig. 4. Conversion as a function of time on stream (TOS) for catalysts prepared using the Al-SnP (a) and GaAl-SnP (b) supports: 10% Ni (■), 15% Ni (○), 20% Ni (▲) and 20% Ni on potassium exchanged supports (▽).

the entrance to small pores producing a decrease in the S_{BET} of 25%. However, it could also be thought that a sintering process took place, but TEM analysis of a spent catalyst discarded this fact, since an increase of metal particle size was not observed. This unchanged metal particle size has also been observed by Huang et al. [7] in the gas-phase hydrogenation of acetonitrile at 383 K after 6 h of TOS on Ru/NaY catalysts.

A key aspect in the study of a particular catalytic reaction is the elucidation of a mechanism which

may explain the results obtained for a family of catalysts. In the case of the gas-phase hydrogenation of acetonitrile, several mechanisms are reported in the literature, but there is still controversial. Thus, the importance of the acid/base nature of the support has been proposed by Verhaak et al. [5] to explain the activity and selectivity of supported nickel catalysts, because it is assumed that the surface acid centers of the support are the reaction sites for condensation reaction leading to higher amines. On the other, some authors [3,9] invoke an influence of the support on the catalytic activity where the metal-support interactions may affect the nature of the nickel particles. They suggest that both the hydrogenation and condensation reactions take place on the metal particles, and the catalytic reaction is sensible to the metal structure. That is, the electronic state of the metal surface is crucial to facilitate the adsorption and activation of the acetonitrile molecules and the intermediate species. However, it is known that the acid properties of the support are responsible of the metal-support interactions, in such a way that a strong interaction will decrease the electronic density on the metal particles.

If we assume that acetonitrile molecules are adsorbed on the metal particles through their lone electron pair with the simultaneous formation of a π back-bonding from the metal to the empty antibonding orbitals of the CN bond, this bond will be weaken, and therefore, easier to hydrogenate. It is observed in Table 5 that conversions increase with the nickel content in both series of catalysts, following the increase in the metal particle size. It arises that the donor character of metal seems to be predominant as the particle size increases. In consequence, the more the electronic density is increased, the ease the desorption of EA which occurs.

By considering the Al-Ni15 and AlK-Ni20 with similar metal particles sizes, it is observed that the latter catalyst exhibit a higher conversion. Since the AlK-Ni20 possesses a lower effective acidity, and the acidity of the support has a strong influence on the electronic density of metal particle, it seems reasonable to take into consideration both the metal surface and the effective acidity of the support in order to explain the observed catalytic behavior. To verify the above assumption, we have plotted in Fig. 5 the selectivity toward EA versus the inverse of the product of the metal surface and the effective acidity of the support (Table 1). It can be observed the good lineal relationship between both parameters, therefore, pointing to that the metal structure seems to be the dominant factor for the hydrogenation and condensation processes.

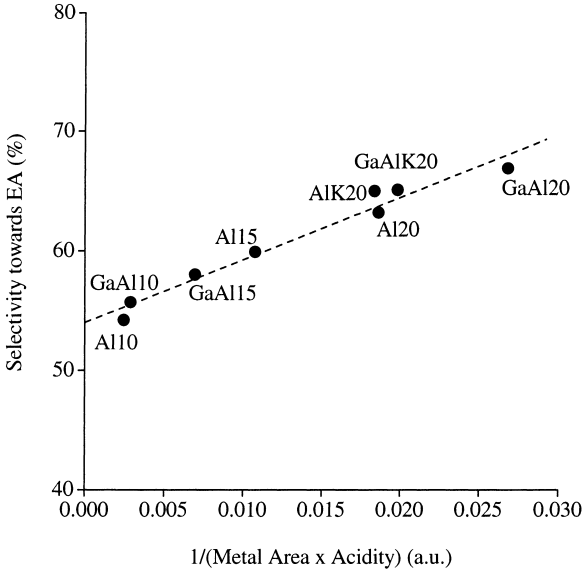

Fig. 5. Relationship between selectivity towards EA and the inverse of the product of metallic surface area and the effective acidity.

4. Conclusions

Nickel supported on alumina- and mixed alumina/gallium oxide-pillared tin phosphates have shown to be active in the gas-phase hydrogenation of acetonitrile at atmospheric pressure. The in situ thermal decomposition of nickel formate has rendered metal nickel particles with sizes comprised between 3 and 42 nm, which depend on both the nickel content and the support. However, the percentage of Ni^0 attained is always lower than 50%. The Ni-based catalysts exhibit, after 5 min of time-on-stream, conversion which reach values >89% for catalysts prepared after treating the support with potassium ions. At 398 K, under the experimental conditions used, this family of catalysts show a selectivity toward EA, at a conversion level of 13.5%, ranging between 54 and 67%, whereas the selectivity toward TEA is always <3%. In all the cases, the catalysts suffer from a severe

deactivation. The catalytic performance observed for these catalysts can be explained on the basis of both the hydrogenation and condensation reactions taking place on the metal particles.

Acknowledgements

We wish to thank the CICYT (Spain) (Project MAT97-906) for financial support. P. Braos-García thanks Junta de Andalucía (Spain) for a fellowship.

References

[1] K. Weissermel, H.J. Arpe, Industrial Organic Chemistry, Verlag Chemie, Berlin, 1978.
[2] M. Grayson (Ed.), Kirk-Othmer Encyclopedia of Chemical Technology, Vol. 2, 2nd Edition, Wiley/Interscience, New York, 1983.
[3] Y. Huang, M.H. Sachtler, Appl. Catal. A: Gen. 182 (1999) 365.
[4] C.V. Rode, M. Arai, M. Shirai, Y. Nishiyama, Appl. Catal. A: Gen. 148 (1997) 405.
[5] M.J.F.M. Verhaak, A.J. van Dillen, J.W. Geus, Catal. Lett. 26 (1994) 37.
[6] F. Medina, R. Dutartre, D. Tichit, B. Coq, N.T. Dung, P. Salagre, J.E. Sueiras, J. Mol. Catal. A: Chem. 119 (1997) 201.
[7] Y. Huang, V. Adeeva, W.M.H. Sachtler, Appl. Catal. A: Gen. 196 (2000) 73.
[8] C.V. Rode, M. Arai, Y. Nishiyama, J. Mol. Catal. A: Chem. 118 (1997) 229.
[9] M. Arai, Y. Takada, Y. Nishiyama, J. Phys. Chem. B 102 (1998) 1968.
[10] T.J. Pinnavaia, Science 220 (1983) 365.
[11] P. Olivera-Pastor, P. Maireles-Torres, E. Rodríguez-Castellón, A. Jiménez-López, T. Cassagneau, D.J. Jones, J. Rozière, Chem. Mater. 8 (1996) 1758.
[12] F.J. Pérez-Reina, E. Rodríguez-Castellón, A. Jiménez-López, Langmuir 15 (1999) 8421.
[13] J. Mérida-Robles, E. Rodríguez-Castellón, A. Jiménez-López, J. Mol. Catal. A: Chem. 145 (1999) 169.
[14] P. Braos-Garcia, E. Rodríguez-Castellón, P. Maireles-Torres, P. Olivera-Pastor, A. Jiménez-López, J. Phys. Chem. B 102 (1998) 1672.
[15] A.B. Edwards, C.D. Garner, K.J. Roberts, J. Phys. Chem. 101 (1997) 20.
[16] M. Wu, D.M. Hercules, J. Phys. Chem. 83 (1979) 2003.
[17] F. Medina-Cabello, D. Tichit, B. Coq, A. Vaccari, N.T. Dung, J. Catal. 167 (1997) 142.
[18] A. Streitwieser, C.H. Heathcock, Química Orgánica, McGraw-Hill Interamericana, 1989, Chapter 23, p.756.
[19] M.J.F.M. Verhaak, A.J. van Dillen, J.W. Geus, J. Catal. 143 (1993) 187.